Handling Missing Data in Limited-View Photoacoustic Tomography Using Compressive Sensing Algorithm-Based Deep Learning

Mary John and Imad Barhumi
College of Engineering, EECE Department
United Arab Emirates University, Al Ain, Abu Dhabi, 15551, UAE
E-mail: {201990198, imad.barhumi}@uaeu.ac.ae

***Abstract*—In photoacoustic tomography, missing sensor data poses a significant challenge for accurate image reconstruction. This study aims to evaluate various imputation methods to address different missing data scenarios, including random missing data, communication loss, and environmental interference. We applied mean imputation, median imputation, k-nearest neighbors (KNN), and multivariate imputation by chained equations (MICE) to these scenarios and assessed their performance using metrics such as MS-SSIM, SSIM, PSNR, R-squared, NMSE, and Entropy. Our results demonstrate that the presence of missing data significantly degrades image quality, with MICE consistently providing the best reconstruction performance across all scenarios. In random missing data cases, MICE achieved the highest SSIM and PSNR values, closely approximating the no missing data scenario. Similar trends were observed in communication loss and environmental interference cases, where MICE outperformed other imputation methods, followed by mean and median imputation, with KNN generally showing the lowest performance. These findings suggest that MICE is a robust method for handling missing data in PAT, enhancing image reconstruction quality.**

Keywords: Photoacoustic Tomography, Compressive Sensing, Deep Learning, Missing Data, Image Reconstruction, Multivariate Imputation by Chained Equations.

I. Introduction

Photoacoustic tomography (PAT) [1] is a hybrid imaging technique that combines the high spatial resolution of optical imaging with the high contrast of ultrasound imaging. It works by illuminating tissue with pulsed laser light, which induces ultrasonic waves due to thermoelastic expansion. These ultrasonic waves are then detected by sensors, and the data is used to reconstruct images of the tissue's optical absorption properties. PAT has shown promise in various biomedical applications, including cancer detection, brain imaging, and functional imaging of blood oxygenation [2].

However, the quality of PAT images heavily depends on the completeness and accuracy of the data acquired by the sensors. In practical scenarios, missing data is a common issue due to various factors such as sensor failures, communication losses, environmental interferences, and scheduled maintenance. These missing data points can degrade the quality of the reconstructed images, making it challenging to achieve accurate diagnostics. To address this, researchers have explored various imputation methods to fill in the missing data before performing image reconstruction.

A. Motivation and Objectives

The primary motivation for this research is to enhance the robustness of PAT image reconstruction in the presence of missing data. Given the critical role of accurate imaging in medical diagnostics, it is essential to develop methods that can effectively handle missing data scenarios and still produce reliable images. This study aims to investigate the effectiveness of various imputation methods—mean, median, KNN, and MICE—in the context of PAT imaging. By simulating practical missing data scenarios, such as random sensor failures, communication losses, and environmental interferences, we seek to evaluate and compare the performance of these imputation methods. Furthermore, we aim to leverage compressive sensing algorithm-based deep learning network, specifically relaxed basis pursuit based on ADMM (Alternating Direction Method of Multipliers) [3], to reconstruct images from the imputed data. This network was initially trained on full-view sensor data and subsequently adapted through transfer learning to handle limited-view semicircular arrangements.

The objectives of this research are:

- To simulate various practical missing data scenarios in PAT.
- To apply and compare different imputation methods for handling missing data.
- To evaluate the performance of these imputation methods using metrics such as MS-SSIM, SSIM, PSNR, R-squared, NMSE, and entropy.
- To demonstrate the effectiveness of deep learning-based image reconstruction method in producing high-quality PAT images from imputed data.
- To provide insights into the strengths and limitations of each imputation method in the context of PAT.

By achieving these objectives, this research aims to contribute to the development of more reliable and robust PAT imaging techniques that can be used in clinical practice, ultimately improving patient outcomes through better diagnostics.

II. Related Works

Handling missing sensor data is a critical challenge in various imaging applications, including PAT. Numerous methods have been developed to address this issue, each with its unique approach and strengths. In [4] a comprehensive review of various imputation methods for missing sensor data is provided, categorizing them based on missingness patterns and properties. This foundational review highlights the diversity of imputation strategies and sets the stage for exploring more advanced techniques. Iterative Imputing Network is introduced in [5], which captures latent temporal dynamics to recover missing sensor data. This method leverages complex temporal patterns, showing significant improvements in applications like air quality and meteorological datasets. In [6] the authors proposed a framework to enhance MICE specifically for large gaps of missing data. Their approach involves reshaping the sensor data to exploit correlations between missing and observed values, splitting the data into extreme and normal values, and building separate MICE models for each. Several machine learning methods for imputing missing sensor data in cardiac imaging datasets are evaluated in [7], including mean imputation, KNN, C4.5 decision trees, and self-organizing maps. This study provides valuable insights into the effectiveness of various imputation techniques in medical imaging contexts. In [8] a novel deep learning-based framework for imputing missing values in sensor data is developed, specifically addressing the challenges of large segment imputation. Their multistage imputation strategy incorporates adaptive evaluation metrics and dynamic data length adjustment. A probabilistic method for imputing missing sensor data in multi-sensory activity recognition, using a conditional Gaussian distribution and exploiting correlation among classifier outputs is proposed in [9]. In [10] an efficient imputation technique based on k-means clustering for IoT sensor networks is presented. Their Best Fit Missing Value Imputation (BFMVI) method partitions incomplete data into clusters, estimates missing values using a random forest model trained on observed data within each cluster, and selects the most suitable imputation technique based on an error score function. These studies highlight the diverse approaches to imputation, from simple statistical methods to sophisticated machine learning techniques, providing a solid foundation for exploring the application of these imputation techniques to PAT imaging to enhance robustness and accuracy of image reconstruction in the presence of missing data.

III. Methodology

This section details the methodology used in our study, encompassing the compressive sensing algorithm, the deep learning network, the simulation of missing data scenarios, and the evaluation metrics employed to assess the performance of the imputation methods and image reconstruction.

A. Compressive Sensing Algorithm and Deep Learning Network

In this study, we employ a compressive sensing (CS) [11] algorithm-based deep learning network to reconstruct PAT images. Specifically, we use a relaxed basis pursuit algorithm based on the ADMM. Compressive sensing leverages the sparsity of signals to reconstruct high-quality images from under-sampled data, making it particularly effective for PAT where complete data acquisition is often challenging.

The significance of the rBP-ADMM (relaxed Basis Pursuit - ADMM) algorithm [12], [13] lies in its ability to address the complex inverse problem in PAT with high efficiency and robustness. The algorithm offers several advantages over traditional methods:

1) Robustness to Noise: rBP-ADMM algorithm integrates regularization terms that mitigate the impact of noise, resulting in more accurate and stable image reconstructions.
2) Iterative Refinement: It iteratively updates the solution, progressively refining the image, which is beneficial for dealing with the ill-posed nature of the PAT inverse problem.
3) Efficient Convergence: By splitting the optimization problem into smaller sub-problems, ADMM framework ensures faster convergence compared to traditional optimization methods, making it suitable for real-time applications.
4) Handling Incomplete Data: It effectively deals with missing or incomplete data, a common issue in practical PAT scenarios due to sensor limitations or failures.

The deep learning network architecture incorporates multiple layers, including convolutional layers, activation functions, and fully connected layers, to facilitate feature extraction and accurate image reconstruction. The network is initially trained on full-view sensor data to learn comprehensive patterns and features. Transfer learning is then applied to adapt the network for limited-view semicircular arrangements, enabling the model to leverage prior knowledge and fine-tuned for scenarios with partial data. The rBP-ADMM algorithm is depicted as in Algorithm 1, where $\mathbf{x}$ is the image to be reconstructed in vectorized form, $\mathbf{y}$ is the pressure sensor data, and $\mathbf{M}$ is the sensing matrix.

Algorithm 1 rBP-ADMM

Require: : $\rho, \alpha, \gamma, r, \tau, \mathbf{y}, \mathbf{M}, k_{\max}$, tol.
  Initialize: $k = 0$, $\mathbf{x}^0 = \mathbf{z}^0 = \mathbf{u}^0 = \mathbf{0}$, NMSE = ∞,
  while $k < k_{\max}$ or NMSE $>$ tol **do**
    $\mathbf{x}^{k+1} \leftarrow \left(\rho\mathbf{I} + \alpha\mathbf{M}^T\mathbf{M}\right)^{-1}\left(\rho\mathbf{z}^k - r\mathbf{u}^k + \alpha\mathbf{M}^T\mathbf{y}\right)$
    $\mathbf{z}^{k+1} \leftarrow S_{\frac{\gamma}{\rho}}\left(\frac{\mathbf{u}^k}{\rho} + \mathbf{x}^{k+1}\right)$
    $\mathbf{u}^{k+1} \leftarrow \mathbf{u}^k + \tau\left(\mathbf{x}^{k+1} - \mathbf{z}^{k+1}\right)$
    NMSE $\leftarrow \frac{\|\mathbf{x}^{k+1} - \mathbf{x}^k\|_2^2}{\|\mathbf{x}^{k+1}\|_2^2}$
    $k \leftarrow k + 1$
  end while
    $\mathbf{x}^* = \mathbf{x}^k$

The unrolled deep learning algorithm, termed U-rBP-ADMM, is designed based on the architecture of the rBP-ADMM algorithm, with iterations transformed into iteration

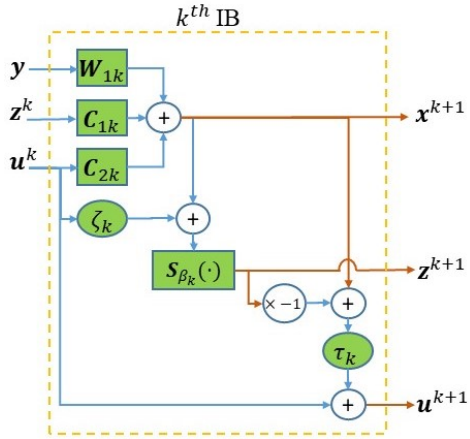

Fig. 1: k^{th} IB in U-rBP-ADMM network diagram.

blocks that perform similar operations to the iterative version using deep network layers. The updates at the $(k+1)$th intermediate block (IB) of the U-rBP-ADMM deep learning network [14] are designed as follows:

$$\mathbf{x}^{k+1} = \mathbf{C}_{1k}\mathbf{z}^k + \mathbf{C}_{2k}\mathbf{u}^k + \mathbf{W}_{1k}\mathbf{y}, \quad (1)$$

$$\mathbf{z}^{k+1} = S_{\beta_k}(\zeta_k\mathbf{u}^k + \mathbf{x}^{k+1}), \quad (2)$$

$$\mathbf{u}^{k+1} = \mathbf{u}^k + \tau_k(\mathbf{x}^{k+1} - \mathbf{z}^{k+1}). \quad (3)$$

Here, $\mathbf{C}_{1k}$ resembles $(\mathbf{I} + \frac{\alpha}{\rho}\mathbf{M}^T\mathbf{M})^{-1}$, $\mathbf{C}_{2k}$ resembles $(\rho\mathbf{I}+\alpha\mathbf{M}^T\mathbf{M})^{-1}r$, and $\mathbf{W}_{1k}$ resembles $(\frac{\rho}{\alpha}\mathbf{I}+\mathbf{M}^T\mathbf{M})^{-1}\mathbf{M}^T$. The matrices $\mathbf{C}_{1k}$ and $\mathbf{C}_{2k}$ are learnable weight matrices. The constant $\frac{1}{\rho}$ is implemented using ζ_k, a learnable parameter. The shrinkage operator with threshold value $\frac{\gamma}{\rho}$ is implemented using the layer $S_{\beta_k}(\cdot)$, with β_k as the learnable threshold value, specific to each IB.

The architecture and iterative updates are visually represented in Figure. 1

B. Simulation of Missing Data Scenarios

To evaluate the performance of the imputation methods, we simulate practical missing data scenarios commonly encountered in PAT and other imaging applications. The following scenarios are considered:

- **Random Sensor Failures**: Sensors can fail randomly due to hardware malfunctions or temporary issues, leading to sporadic missing data across the sensor array. To simulate this, we randomly set a certain percentage of data points to zero. For instance, if 10% of the data is considered missing, we randomly select 10% of the total data points and set their values to zero.
- **Temporary Communication Loss**: Intermittent communication issues can cause temporary loss of data from certain sensors. It simulated by setting blocks of 10 consecutive samples to zero across all sensors to mimic temporary communication interruptions. This method resulted in approximately 14.29% of the data being set to zero, helping to analyze the impact of systematic data loss on image reconstruction quality.
- **Environmental Interference**: Environmental factors such as obstructions or external noise can interfere with certain sensors, causing localized data loss. Environmental interference was simulated by setting data for specific sensors (5, 15, and 25) to zero for samples 30 to 45, mimicking interference in localized regions. This resulted in approximately 8% of the sensor data being lost.

These scenarios help in understanding the impact of different types of missing data on the reconstruction quality and the effectiveness of various imputation methods.

C. Imputation Methods

To address the missing data in the simulated scenarios, we employ and compare several imputation methods:

- **Mean Imputation**: This simple technique involves replacing missing data points with the mean value of the observed data. Although it is easy to implement, it does not account for the relationships between data points and can introduce bias.
- **Median Imputation**: Similar to mean imputation, but missing values are replaced with the median of the observed data. Median imputation is more robust to outliers compared to mean imputation.
- **KNN Imputation**: KNN imputation replaces missing values based on the k-nearest neighbors' observed data points. This method considers the relationships between data points and can provide more accurate imputations than mean or median imputation.
- **MICE**: MICE is an advanced imputation technique that performs multiple imputations by creating several plausible imputed datasets and then averaging the results. It accounts for the uncertainty around missing values and leverages the correlations among data points.

These methods are applied to the simulated datasets to fill in the missing values, and their performance is compared in terms of reconstruction quality.

D. Evaluation Metrics

To assess the performance of the imputation methods and the overall image reconstruction quality, we use the following evaluation metrics:

- **Multi-Scale Structural Similarity Index (MS-SSIM)**: MS-SSIM evaluates the structural similarity between the reconstructed image and the original image at multiple scales. It provides a comprehensive measure of image quality by considering luminance, contrast, and structural information.
- **Structural Similarity Index (SSIM)**: SSIM measures the similarity between two images based on luminance, contrast, and structure. It is a widely used metric for assessing image quality and is sensitive to changes in image structure.

- **Peak Signal-to-Noise Ratio (PSNR)**: PSNR measures the ratio between the maximum possible value of a signal and the power of corrupting noise. It is commonly used to evaluate the quality of reconstructed images, with higher values indicating better quality.
- **R-squared (R^2)**: R^2 quantifies the proportion of variance in the observed data that is predictable from the reconstructed data. It is a measure of goodness-of-fit, with values closer to 1 indicating better fit.
- **Normalized Mean Squared Error (NMSE)**: NMSE measures the mean squared error between the reconstructed and original images, normalized by the variance of the original image. Lower values indicate better reconstruction accuracy.
- **Entropy**: Entropy measures the randomness or complexity of the image. In the context of image reconstruction, it provides insights into the information content and quality of the reconstructed image.

These metrics provide a comprehensive evaluation of the imputation methods and the overall performance of the image reconstruction process. By comparing the results across different imputation techniques and missing data scenarios, we aim to identify the most effective methods for handling missing data in limited-view circle sensor arrangements in PAT imaging.

IV. Experimental Results

This section presents the experimental results obtained from the proposed methodology. We evaluate the performance of the imputation methods under various missing data scenarios and assess the reconstruction quality of PAT images using the proposed deep learning network.

A. Experimental Setup

The experiments were conducted using a limited-view semicircle sensor arrangement, as shown in Figure 2. The setup consists of 71 sensors arranged in a semicircular pattern, capturing 75 samples each. This arrangement simulates practical scenarios [15] where complete circular data acquisition is not feasible.

The data used for the experiments was subjected to different missing data scenarios, including random sensor failures, temporary communication loss, and environmental interference. The missing data was then imputed using various imputation methods such as mean, median, KNN, and MICE. The imputed data was subsequently fed into the trained deep learning network to reconstruct the PAT images. The performance analysis were conducted to reconstruct three test images as shown in Figure 3.

B. Results and Discussion

Analysis of the three cases of practical missing data scenarios are discussed in this section. Table I presents the results for Images 1, 2, and 3 with random data missing, communication loss, and environmental interference. The "No missing" case, where there is no missing data, serves as the reference for optimal image reconstruction quality.

TABLE I: U-rBP-ADMM performance with missing data.

Case	MS-SSIM	SSIM	PSNR	R^2	NMSE	Entropy
Random Data Missing						
Image 1						
No missing	0.9730	0.7768	31.99	0.9652	0.01968	5.664
Missing	0.9455	0.6529	28.27	0.9213	0.04454	5.725
Mean Imputed	0.9599	0.6943	29.91	0.9469	0.03007	5.797
Median Imputed	0.9598	0.6968	29.88	0.9455	0.03086	5.726
KNN Imputed	0.9415	0.6379	28.61	0.9297	0.03981	5.961
MICE Imputed	0.9664	0.7411	31.13	0.9573	0.02420	5.668
Image 2						
No missing	0.9627	0.7130	30.01	0.9654	0.02020	6.128
Missing	0.9313	0.5917	26.54	0.9262	0.04305	6.134
Mean Imputed	0.9487	0.6312	28.24	0.9501	0.02910	6.246
Median Imputed	0.9492	0.6387	28.31	0.9496	0.02936	6.129
KNN Imputed	0.9088	0.5315	25.78	0.9140	0.05016	6.425
MICE Imputed	0.9570	0.6857	29.27	0.9596	0.02355	6.199
Image 3						
No missing	0.9505	0.6433	28.42	0.9369	0.04489	5.320
Missing	0.9146	0.5313	26.25	0.8984	0.07235	5.395
Mean Imputed	0.9295	0.5545	27.08	0.9182	0.05826	5.510
Median Imputed	0.9275	0.5558	27.01	0.9155	0.06018	5.448
KNN Imputed	0.9132	0.5243	26.51	0.9058	0.06707	5.532
MICE Imputed	0.9409	0.6017	27.84	0.9281	0.05116	5.343
Communication Loss						
Image 1						
Missing	0.8973	0.5496	25.34	0.8498	0.08505	5.797
Mean Imputed	0.9279	0.6186	27.66	0.9140	0.04867	5.991
Median Imputed	0.9317	0.6264	27.85	0.9160	0.04755	5.882
KNN Imputed	0.8846	0.5334	25.70	0.8655	0.07614	6.099
MICE Imputed	0.9161	0.5601	27.77	0.9051	0.05374	5.847
Image 2						
Missing	0.8822	0.4844	23.78	0.8607	0.08121	6.146
Mean Imputed	0.9151	0.5397	25.58	0.9106	0.05213	6.328
Median Imputed	0.9197	0.5511	25.65	0.9104	0.05225	6.224
KNN Imputed	0.8443	0.4482	23.03	0.8407	0.09289	6.445
MICE Imputed	0.8757	0.4701	24.54	0.8821	0.06873	6.334
Image 3						
Missing	0.8906	0.4714	25.01	0.8616	0.09850	5.323
Mean Imputed	0.9133	0.5092	26.42	0.9057	0.06715	5.624
Median Imputed	0.9110	0.5156	26.21	0.9000	0.07122	5.548
KNN Imputed	0.8859	0.4660	24.95	0.8679	0.09405	5.664
MICE Imputed	0.8909	0.4614	25.54	0.8801	0.08537	5.719
Environmental Interference						
Image 1						
Missing	0.9665	0.7540	31.13	0.9580	0.02376	5.645
Mean Imputed	0.9685	0.7533	31.66	0.9627	0.02111	5.710
Median Imputed	0.9697	0.7582	31.72	0.9632	0.02084	5.699
KNN Imputed	0.9575	0.7225	31.02	0.9572	0.02422	5.764
MICE Imputed	0.9523	0.7066	30.67	0.9515	0.02745	5.744
Image 2						
Missing	0.9570	0.6920	29.56	0.9614	0.02252	6.084
Mean Imputed	0.9564	0.6833	29.64	0.9625	0.02189	6.132
Median Imputed	0.9590	0.6936	29.77	0.9634	0.02136	6.120
KNN Imputed	0.9181	0.6073	27.31	0.9372	0.03662	6.222
MICE Imputed	0.9093	0.5921	26.89	0.9285	0.04167	6.227
Image 3						
Missing	0.9489	0.6353	28.37	0.9360	0.04559	5.304
Mean Imputed	0.9468	0.6221	28.25	0.9348	0.04640	5.380
Median Imputed	0.9458	0.6175	28.23	0.9343	0.04677	5.376
KNN Imputed	0.9469	0.6228	28.27	0.9349	0.04634	5.358
MICE Imputed	0.9469	0.6251	28.35	0.9349	0.04634	5.303

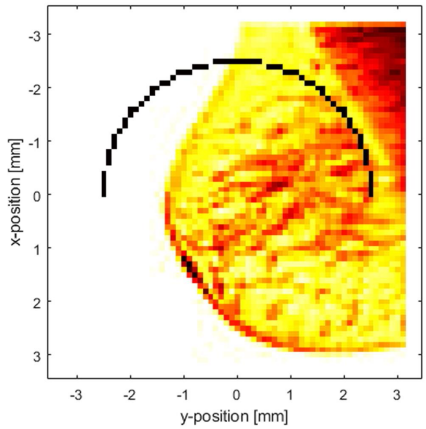

Fig. 2: Limited-View semicircle sensor arrangement.

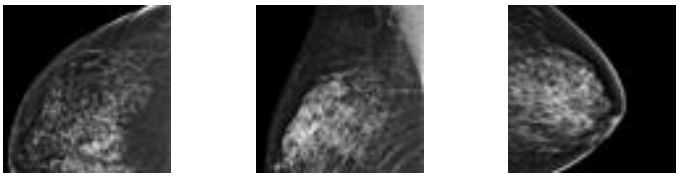

(a) Image 1 (b) Image 2 (c) Image 3

Fig. 3: Test images.

1) Random Data Missing: The "No missing" case consistently shows the highest values across all metrics, indicating the best quality reconstruction. In the presence of missing data, there is a significant drop in image quality. Among the imputation methods, the "MICE Imputed" case provides the best performance overall, closely related to the no missing data scenario. For instance, in Image 1, the "No missing" case has the highest MS-SSIM (0.9730), SSIM (0.7768), PSNR (31.99), and R-squared (0.9652), and the lowest NMSE (0.01968) and Entropy (5.664). The "MICE Imputed" case shows the best performance among the imputed cases, with MS-SSIM of 0.9664, SSIM of 0.7411, and PSNR of 31.13. The "Mean Imputed" and "Median Imputed" cases show comparable performance, demonstrating noticeable improvement over the missing data case but not reaching the level of MICE imputation. The "KNN Imputed" case generally shows the lowest performance among the imputation methods tested.

2) Communication Loss: Among the imputation methods evaluated, the "MICE Imputed" method consistently yielded the best results, closely resembling the no missing data scenario. For example, in Image 1, the "MICE Imputed" case achieved the highest MS-SSIM (0.9161), SSIM (0.5601), PSNR (27.77), R-squared (0.9051), and maintained a lower Entropy (5.847) compared to other imputation methods. The "Mean Imputed" and "Median Imputed" methods showed comparable performance, typically being the second-best and third-best methods, respectively. They improved image quality over the "Missing" case but did not perform as well as MICE. The "KNN Imputed" method consistently showed the lowest performance among the imputation methods tested, indicating its relative ineffectiveness in handling communication loss scenarios.

3) Environmental Interference: From the analysis of all images, it is clear that the "MICE Imputed" method consistently provides the best results, closely approximating the no missing data scenario. For example, in **Image 1**, the "MICE Imputed" case achieves the highest performance with MS-SSIM of 0.9523, SSIM of 0.7066, PSNR of 30.67, R-squared of 0.9515, and entropy of 5.744. The "Mean Imputed" and "Median Imputed" cases also show substantial improvements over the missing data scenario, with "Median Imputed" slightly outperforming "Mean Imputed". The "KNN Imputed" case generally shows the least effective performance, often close to or slightly better than the "Missing" data case.

Overall, from the analysis, it is evident that missing data, whether from random data loss, communication loss, or environmental interference, significantly impacts the quality of image reconstruction in photoacoustic tomography. In all scenarios, the "No missing" data case provides the best image reconstruction quality across all images. When data is missing, there is a substantial drop in image quality. Among the imputation methods, "MICE Imputed" consistently yields the best results, closely approximating the no missing data case in all types of missing data scenarios. The "Mean Imputed" and "Median Imputed" cases show comparable results, better than the missing data scenario but not as good as MICE. The "KNN Imputed" case generally shows the lowest performance among the imputation methods tested. While environmental interference impacts image quality, its effect is less severe compared to random data loss and communication loss. Overall, "MICE Imputed" emerges as the most effective imputation method, followed by "Mean Imputed" and "Median Imputed," with "KNN Imputed" being the least effective.

V. Conclusion

In this study, we evaluated the effectiveness of various imputation methods—mean imputation, median imputation, KNN, and MICE for handling missing sensor data in PAT under different scenarios: random missing data, communication loss, and environmental interference. Our findings indicate that missing data significantly degrades image reconstruction quality in PAT. Among the tested imputation methods, MICE consistently outperformed others, yielding the best image reconstruction metrics across all scenarios. Mean and median imputations provided moderate improvements, while KNN generally exhibited the lowest performance. These results highlight the importance of selecting robust imputation strategies, such as MICE, to mitigate the impact of missing data on PAT imaging. Future research should explore further optimization of imputation techniques and their application to various imaging contexts.

References

[1] Wang, Lihong V. "Prospects of photoacoustic tomography." *Medical Physics*, vol. 35, no. 12, 2008, pp. 5758–5767. Wiley Online Library.

[2] Gu, Yanru, Sun, Yuanyuan, Wang, Xiao, Li, Hongyu, Qiu, Jianfeng, and Lu, Weizhao. "Application of photoacoustic computed tomography in biomedical imaging: A literature review." *Bioengineering & Translational Medicine*, vol. 8, no. 2, 2023, p. e10419. Wiley Online Library.

[3] Nishihara, Robert, Lessard, Laurent, Recht, Ben, Packard, Andrew, and Jordan, Michael. "A general analysis of the convergence of ADMM." In *International Conference on Machine Learning*, 2015, pp. 343–352. PMLR.

[4] R. N. Faizin, M. Riasetiawan, and A. Ashari, "A review of missing sensor data imputation methods," in *2019 5th International Conference on Science and Technology (ICST)*, vol. 1, pp. 1–6, 2019.

[5] J. Zhou and Z. Huang, "Recover Missing Sensor Data with Iterative Imputing Network," *ArXiv*, vol. abs/1711.07878, 2017. [Online]. Available: https://api.semanticscholar.org/CorpusID:30222955

[6] R. Wu, S. D. Hamshaw, L. Yang, D. W. Kincaid, R. Etheridge, and A. Ghasemkhani, "Data imputation for multivariate time series sensor data with large gaps of missing data," *IEEE Sensors Journal*, vol. 22, no. 11, pp. 10671–10683, 2022.

[7] Y. Liu and V. Gopalakrishnan, "An overview and evaluation of recent machine learning imputation methods using cardiac imaging data," *Data*, vol. 2, no. 1, p. 8, 2017.

[8] J. Yang, Y. Shao, C. Li, and W. Wang, "A multistage deep imputation framework for missing values large segment imputation with statistical metrics," *Applied Soft Computing*, vol. 146, p. 110654, 2023.

[9] H. Sagha, J. R. Millán, and R. Chavarriaga, "A Probabilistic Approach to Handle Missing Data for Multi-Sensory Activity Recognition," in *Ubiquitous Computing*, 2010. [Online]. Available: https://api.semanticscholar.org/CorpusID:12966009

[10] B. Agbo, H. Al-Aqrabi, R. Hill, and T. Alsboui, "Missing data imputation in the Internet of Things sensor networks," *Future Internet*, vol. 14, no. 5, p. 143, 2022.

[11] D. L. Donoho, "Compressed sensing," *IEEE Transactions on information theory*, vol. 52, no. 4, pp. 1289–1306, 2006.

[12] M. J. John and I. Barhumi, "Fast and efficient pat image reconstruction algorithms: A comparative performance analysis," *Signal Processing*, vol. 201, p. 108691, 2022.

[13] Chen, Shaobing, and Donoho, David. "Basis pursuit." In *Proceedings of 1994 28th Asilomar Conference on Signals, Systems and Computers*, vol. 1, 1994, pp. 41–44. IEEE.

[14] M. John and I. Barhumi, "Advancing Sensor-Data Based PAT Image Reconstruction Through Efficient and Intelligible Unrolled Networks," *IEEE Access*, vol. 11, pp. 117053–117066, 2023.

[15] John, Mary Josy, and Barhumi, Imad. "Compressive Sensing Based Algorithms for Limited-View PAT Image Reconstruction." In *2023 Asia Pacific Signal and Information Processing Association Annual Summit and Conference (APSIPA ASC)*, 2023, pp. 1317–1322. IEEE.